ELSEVIER

Biochimica et Biophysica Acta 1564 (2002) 435–448

BIOCHIMICA ET BIOPHYSICA ACTA
BBA

www.bba-direct.com

Determination of membrane protein topology by red-edge excitation shift analysis: application to the membrane-bound colicin E1 channel peptide

Monica C. Tory [1], A. Rod Merrill *

Department of Chemistry and Biochemistry, Guelph-Waterloo Centre for Graduate Work in Chemistry, University of Guelph, Guelph, ON, Canada N1G 2W1

Received 25 March 2002; received in revised form 18 June 2002; accepted 20 June 2002

Abstract

A new approach for the determination of the bilayer location of Trp residues in proteins has been applied to the study of the membrane topology of the channel-forming bacteriocin, colicin E1. This method, red-edge excitation shift (REES) analysis, was initially applied to the study of 12 single Trp-containing channel peptides of colicin E1 in the soluble state in aqueous medium. Notably, REES was observed for most of the channel peptides in aqueous solution upon low pH activation. The extent of REES was subsequently characterized using a model membrane system composed of the tripeptide, Lys-Trp-Lys, bound to dimyristoyl-*sn*-glycerol-3-phosphatidylserine liposomes. Subsequently, data accrued from the model peptide–lipid system was used to interpret information obtained on the channel peptides when bound to dioleoyl-*sn*-glycerol-3-phosphatidylcholine/dioleoyl-*sn*-glycerol-3-phosphatidylglycerol membrane vesicles. The single Trp mutant peptides were divided into three categories based on the change in the REES values observed for the Trp residues when the peptides were bound to liposomes as compared to the REES values measured for the soluble peptides. F-404W, F-413W, F-443W, F-484W, and W-495 peptides exhibited small and/or insignificant REES changes (ΔREES) whereas W-424, F-431W, and Y-507W channel peptides possessed modest REES changes (3 nm≤ΔREES≤7 nm). In contrast, wild-type, Y-367W, W-460, Y-478W, and I-499W channel peptides showed large ΔREES values upon membrane binding (7 nm<ΔREES≤12 nm). The REES data for the membrane-bound structure of the colicin E1 channel peptide proved consistent with previous data for the topology of the closed channel state, which lends further credence to the currently proposed channel model. In conclusion, the REES method provides another source of topological data for assignment of the bilayer location for Trp residues within membrane-associated proteins; however, it also requires careful interpretation of spectral data in combination with structural information on the proteins being investigated.

Keywords: Tryptophan fluorescence; Membrane interaction; Channel structure

1. Introduction

The cytotoxic function of the bactericidal protein, colicin E1, is found in the ability of the protein to form voltage-gated, ion-conductive channels within the cytoplasmic membrane of susceptible cells. However, despite recent strides in the elucidation of the soluble structures of whole colicin [1] and various channel-domain fragments [2–4], the current state of knowledge of the structure and function of membrane-associated colicins is modest at best. Colicin E1, secreted by *Escherichia coli* that possess the naturally occurring *colE1* plasmid, consists of three functional domains, the translocation, receptor-binding, and channel-forming domains. Initially, the receptor-binding domain [5] interacts with the vitamin B_{12} receptor of target cells [6]. Following recognition, the translocation domain interacts

Abbreviations: λ_{em}max, wavelength of maximum fluorescence emission; ANS, 1-anilinonaphthalene-8-sulfonic acid; DMG, dimethylglutarate; DMPC, dimyristoyl-*sn*-glycerol-3-phosphatidylcholine; DMPS, dimyristoyl-*sn*-glycerol-3-phosphatidylserine; DOPC, dioleoyl-*sn*-glycerol-3-phosphatidylcholine; DOPG, dioleoyl-*sn*-glycerol-3-phosphatidylglycerol; ESR, electron spin resonance; LUV, large unilamellar vesicle; NATA, *N*-acetyl-L-tryptophanamide; NAYA, *N*-acetyl-L-tyrosinamide; NBD, *N*-(7-nitrobenz-2-oxa-1,3-diazol); NBD-PE, *N*-(7-nitrobenz-2-oxa-1,3-diazol-4-yl)-1,2-dipalmitoyl-*sn*-glycero-phosphoethanolamine; REES, red-edge excitation shift; T_m, phase transition temperature; TNS, 2-(*p*-toluidinyl)-naphthalene-6 sulfonic acid; Trp^-, Trp-deficient peptide

* Corresponding author. Tel.: +1-519-8244120; fax: +1-519-7661499.
E-mail address: merrill@chembio.uoguelph.ca (A. Rod Merrill).
[1] Present address: Pharmacia Corporation, Cell and Molecular Biology, 30-1 Henrieta St., Kalamazoo, MI 49001, USA.

0005-2736/02/$ - see front matter © 2002 Elsevier Science B.V. All rights reserved.
PII: S0005-2736(02)00493-5

with the *tolA* gene product, which permits the translocation of colicin E1 across the outer membrane, and into the periplasm [7]. In the periplasm, the channel domain undergoes a conformational change to an insertion-competent state, then inserts spontaneously into the cytoplasmic membrane, forming an ion channel. The channel translocates monovalent ions, resulting in the dissipation of the cationic gradients (H^+, K^+, Na^+) of the cell, causing depolarization of the cytoplasmic membrane [8,9]. In an effort to compensate for the membrane depolarization effected by the colicin E1 channel, Na^+/K^+ ATPase activity is increased in the target cell, resulting in the consumption of ATP reserves, without concomitant replenishment [10]. The final outcome is host cell death.

Colicin E1 is one member of the family of colicins (including A, Ia, Ib, B and N) that form dissipative ion channels in the cytoplasmic membrane of susceptible *E. coli* cells [11]. Two members of this family, colicin A and E1, have been extensively studied in their membrane-bound states and their channel properties have been thoroughly investigated [11,12]. A number of techniques have been used to study the topology of the membrane-bound state of colicin E1. Studies of the surface topology of the colicin E1 channel peptide bound to liposomes have been performed using proteases [13]. These investigators showed that the bound polypeptide is largely sensitized to trypsin proteolysis relative to that in aqueous solution. The *N*-terminal one-third of the 190-residue membrane-bound colicin E1 channel peptide is unbound or loosely bound with the C-terminal two-thirds showing little sensitivity to protease. Saturation mutagenesis of helices 8 and 9, in which 29 mutations were made at 26 different sites, indicated that the hydrophobic anchor domain (A-471 to I-508) comprises a pair of hydrophobic helices that spans the membrane bilayer [14]. The membrane-associated closed state of the channel was also studied by depth-dependent fluorescence quenching [15]. This approach used Trp as the reporter spectroscopic probe and doxyl-labeled phospholipids as the quencher species. The results from this study were consistent with the presence of only two *trans*-membrane segments in the closed channel and were in agreement with those obtained by Song et al. [14] and by Shin et al. [16]—the latter involved an electron spin resonance (ESR) study of spin-labeled cysteine mutants of the channel peptide. Furthermore, the structure and dynamics of the gating mechanism of the colicin E1 channel were previously studied by hydrophobic photolabeling [17] and by site-specific biotinylation [18]. Also, the membrane-bound volume of the colicin E1 channel peptide was determined using light scattering analysis and was found to be 177 nm^3, suggesting that the peptide likely has a large hydration shell when membrane bound [19]. Recently, Zakharov et al. [20] proposed that the membrane-bound state of the colicin E1 channel peptide (closed channel) exists as a two-dimensional helical array with most of the helices appressed closely to the bilayer surface. Also, Kim et al. [21] used ^{15}N-labelled P190 colicin in oriented planar phospholipid bilayers and found that the data were consistent with a single *trans*-membrane helical hairpin inserted into the bilayer from each colicin molecule. Tory and Merrill [22] used acrylamide quenching of intrinsic fluorescence of engineered mutant proteins to determine the membrane-bound topology of the colicin E1 peptide. Recently, Nardi et al. [23] revisited the issue of the shortest channel fragment that is able to form a functional ion channel in colicin A. It was shown that the C-terminal one-half (helices 5–10) are all that is necessary for the formation of both an in vitro and in vivo active channel, yet again confirming the pore-forming colicin enigmatic dogma that "there is not enough monomeric protein to form the channel." Moreover, Zakharov et al. [24] characterized the kinetic steps involved in the binding and insertion process for the colicin channel domain. A general mechanism for toxin insertion into membranes was suggested by Elkins et al. [3] based on comparison of the X-ray structures of the soluble channel peptides of colicin A and E1.

To achieve a complete understanding of the structure–function relationships within organized macromolecular complexes, for example membrane-associated proteins, the dynamics of both the constituent molecules and the entire system must be investigated. Fluorescence spectroscopy is ideal for studying such systems, since it yields both structural and dynamic information and is a noninvasive, sensitive technique that occurs on a time scale that is suitable for studying a large array of molecular events.

In the present study, the nature of interaction with the polar solvent and/or head group structure of model membranes by Trp residues within 12 single Trp mutant peptides of colicin E1 was probed using red-edge excitation. The basic premise for this spectroscopic approach to the study of membrane-bound proteins is that the fluorescence emission maxima (λ_{em}max) and anisotropy values of tryptophan residues may exhibit red-edge excitation shift (REES) under certain conditions, which can be used as a measure of the relative mobility of dipolar solvent (water, protein or phospholipid headgroup components) in the region of the fluorophore. This may provide additional information about the relative motional restriction of regions of the colicin E1 peptide in both the soluble and membrane-bound states, and may help to provide further insight into the intriguing channel structure of the pore-forming colicins.

2. Materials and methods

2.1. Red edge excitation shift—theory and application

Generally, the emission spectrum of a fluorophore is independent of the excitation wavelength and as such, this principle is often used as an indication of the purity and/or homogeneity of a fluorescent sample. Thus, for most fluorophores in fluid solvents, the emission spectra are independent of excitation wavelength and solvent viscosity [25].

However, it has been observed that in moderately polar and viscous solvents, the emission spectra of polar fluorophores may shift to longer wavelengths as the excitation wavelength is increased toward the red side (longer wavelength) of the absorption profile for the probe [26,27].

An explanation for the wavelength-dependence of the excitation spectrum for polar fluorophores in polar, viscous solvents is illustrated in Fig. 1A (based on a two-state model). Excitation at a wavelength central to the absorption band (λ) is assumed to yield an initially excited state (F) around which solvent reorientation has not occurred. The F state can decay to a lower energy state (R) with a reorientation lifetime (τ_S). The rate of relaxation is determined by the nature of the interactions between the fluorophore and the surrounding solvent molecules and the rate at which these interactions are affected by the new excited state dipole moment [25]. Although solvent relaxation is more complex than described by a simple two-state model, this model provides a simple conceptual framework to explain the observed effects of red-edge excitation.

The emission from the F state ($h\nu_1$) is centered at shorter wavelengths (λ) relative to that of the R state ($h\nu_2$). Now, if we designate the direct excitation of the F state as Ex(F) and the excitation of the R state as Ex(R) (where Ex(R)λ>Ex(F)λ), then three possibilities exist (Fig. 1B–D). The first is when the solvent reorientation time is much shorter than the fluorescence lifetime of the fluorophore ($\tau_S\tau_F$, Fig. 1B); the solvent molecules have sufficient

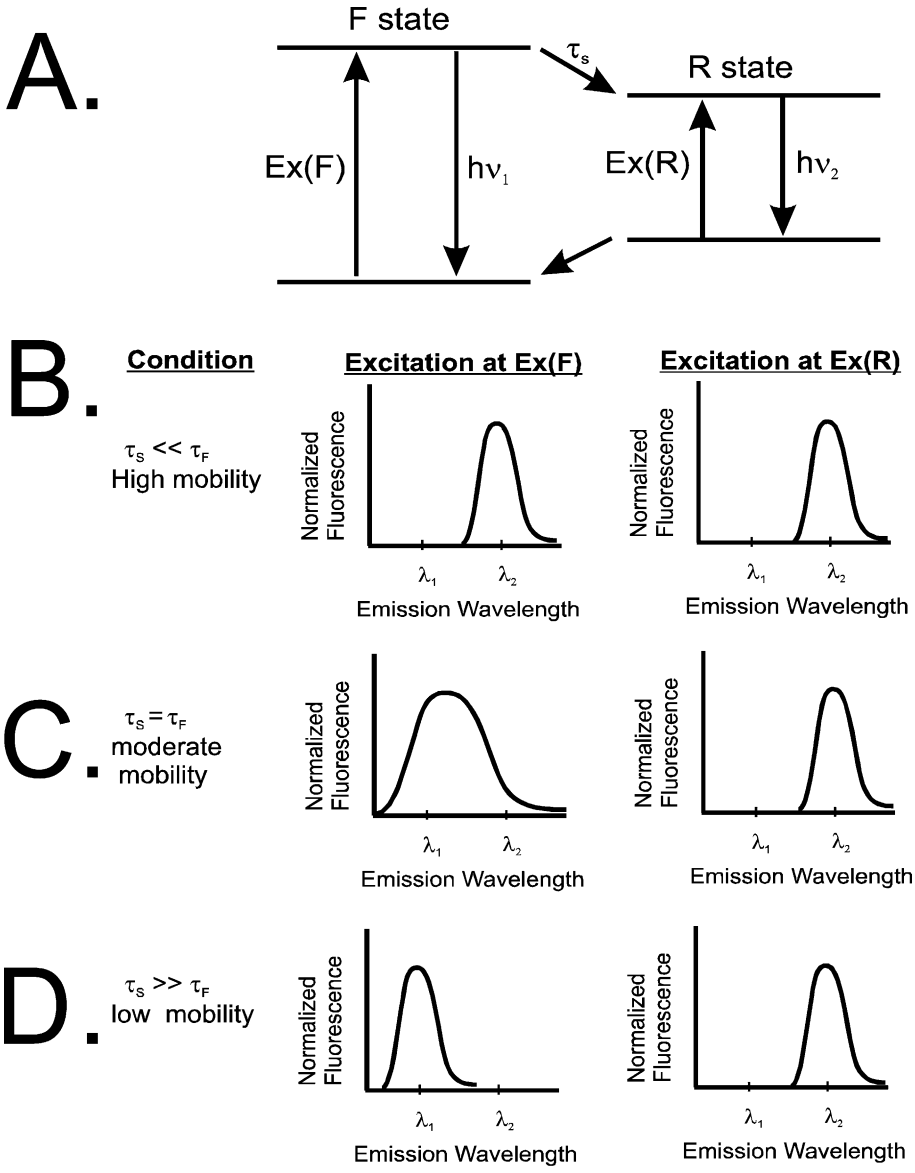

Fig. 1. Two-state model for solvent relaxation in terms of (A) energy levels and (B–D) spectra. The F and R states refer to the Franck–Condon (initial) and relaxed (or final) excited states, respectively. The τ_F is the lifetime of the fluorophore and τ_S is the reorientation time of the solvent molecules. Ex(F) and Ex(R) are the respective wavelengths associated with direct excitation of the Franck–Condon (F) and relaxed states (R) (figure was modified from Ref. [39]).

time to reorient before the fluorophore emits. Therefore, the relaxed emission is observed and is independent of the excitation wavelength used (Ex(F) or Ex(R)). Under these conditions, excitation of either the F state or the R state yields emission spectra centered at λ_2. This situation would be expected for a fluorophore in bulk, nonviscous solvents or at elevated temperatures. The second possibility is the situation where the rate of solvent reorientation is comparable to the fluorescence lifetime ($\tau_S \cong \tau_F$, Fig. 1C), conditions of intermediate viscosity or temperature. In this instance, excitation at Ex(F) gives rise to a spectrum centered at a wavelength intermediate between λ_1 and λ_2. Although the F state is initially excited, the comparable values of the τ_F and τ_R give rise to emissions from both F and R states. Such an inhomogeneous spectrum also has a wider spectral distribution. However, upon red-edge excitation (Ex(R)), the emission occurs mainly from the R state, giving rise to a more red-shifted emission spectrum with a more narrow spectral distribution and which is composed of emission predominantly from the R state [27,28]. The third possibility occurs when the fluorophore is found in a more viscous medium or at very low temperatures. In this case, the relaxation time (a function of the rate of physical reorientation of the solvent molecules) is markedly increased and is now much longer than the fluorescence lifetime ($\tau_S \gg \tau_F$, Fig. 1D). Under these conditions, the emission will be excitation dependent; the blue-shifted emission of the F state (emission maximum at λ_1) is observed with normal excitation (Ex(F)). However, if the system is excited with lower energy (Ex(R)), it will select a subset of the fluorophore population around which the solvent dipoles are oriented so as to decrease the energy difference between the ground and the excited states. In other words, the photoselected ground state is higher in energy relative to the photoselected excited state due to the alignment of solvent dipoles in the latter, which has a solvent-relaxed orientation. Accordingly, red-edge excitation under these conditions selects those molecules that have a solvent-relaxed environment and will exhibit red-shifted absorption and emission spectra (emission spectrum is centered at λ_2).

In summary, these red shifts in the fluorescence emission spectrum of a fluorophore occur because long wavelength excitation results in photoselection of those fluorophores that are interacting most strongly with the polar solvent molecules. Thus, the observation of REES requires that these enhanced dipole–dipole interactions be maintained in the photoselected population during the lifetime of the excited state. Therefore, the extent of the REES effect depends upon the dynamic properties of the environment surrounding the fluorophore, in addition to the solvent polarity and the sensitivity of the fluorophore to the dipolar solvent such as water. Previously, Lakowicz and Keating-Nakamoto [25] demonstrated that this type of spectral shift indicates that REES results in the selective excitation of "solvent-relaxed" fluorophores. Polar fluorophores in nonpolar solvents usually do not exhibit REES nor do nonpolar fluorophores in polar solvents but it is a property of polar fluorophores in polar solvents and requires the presence of a highly viscous interface such as a membrane bilayer [28]. Accordingly, it has been proposed that REES effects can be used to localize polar fluorophores at the membrane bilayer interface, where solvent mobility is restricted [25,28].

2.2. Preparation and purification of colicin E1 channel peptides

Twelve single Trp-containing mutants of colicin E1, a mutant without Trp residues (Trp^-), and wild-type colicin E1 were prepared and purified as described previously [29,30]. Protein concentrations were determined for mutant and wild-type channel peptides using molar extinction coefficients as determined previously [29].

2.3. Preparation of vesicles

Large unilamellar vesicles (LUVs) composed of either 60:40 (mol/mol) 1,2-dioleoyl-*sn*-glycerol-3-phosphatidylcholine (DOPC) and 1,2-dioleoyl-*sn*-glycerol-3-phosphatidylglycerol (Avanti Polar Lipids, Birmingham, AL), or dimyristoyl-*sn*-glycerol-3-phosphatidylserine were prepared as described previously [15] using a hand-held extruder (Liposofast™, Avestin Inc., Ottawa, Canada). Light scattering analysis [19] was used to determine the mean radius of the liposomes (53±9 nm). Phospholipid concentration was determined using a microBartlett assay [31], following degradation of the phospholipids by ashing in $Mg(NO_3)_2$ [32].

2.4. Fluorescence measurements

Fluorescence spectroscopic measurements were performed using a PTI Alphascan-2 spectrofluorometer (Photon Technology Inc., South Brunswick, NJ) equipped with a thermostated cell holder, holographic excitation grating and appropriate emission cut-off filters as required (Oriel Corporation, Stratford, CT).

Membrane-associated samples were prepared by adding 16.7 μg/ml LUVs to 1.3 μM colicin E1 channel peptide in 10 mM dimethylglutarate (DMG), 100 mM NaCl, pH 3.5 in a 0.5 cm quartz cuvette. A sample blank containing LUVs only was prepared to correct for vesicle-induced light scattering. Another blank solution, used to correct for the contribution of fluorescence emission arising from tyrosine residues, contained Trp^- colicin E1 channel peptide mixed with LUVs as specified above. The samples were equilibrated for 10 min with intermittent mixing by inversion of the stoppered cuvettes, prior to spectroscopic measurement.

Soluble samples (no vesicles) for fluorescence measurement contained 16.9 μM colicin E1 channel peptide in 10 mM DMG, 100 mM NaCl, pH 3.5 in 600 μl of solution. A blank containing Trp^- colicin E1 channel peptide (16.9 μM)

in 10 mM DMG, 100 mM NaCl, pH 3.5, was used to correct for the contribution of tyrosine fluorescence to the total fluorescence emission signal. Control samples were composed of (i) *N*-acetyl-L-tryptophanamide (NATA, Sigma Chemical Co., St. Louis, MO) and (ii) 9:1 (mol/mol) *N*-acetyl-L-tyrosinamide (NAYA, Sigma)/NATA in 10 mM DMG, 100 mM NaCl, pH 3.5.

2.5. Fluorescence emission spectra

For each sample, fluorescence emission spectra were collected using excitation wavelengths of 287.5, 290.0, 292.5, 295.0, 297.5, and 300 nm while scanning the emission wavelength range from 310 through 425 nm with 0.5-nm steps. The excitation and emission slits were 4 and 6 nm, respectively. For samples containing LUVs, cutoff filters ($\lambda \leq 299$ nm for $\lambda_{ex} \leq 295$ nm, $\lambda \leq 310$ nm for $\lambda_{ex} > 295$ nm) were placed in the emission beam in front of the entrance window of the emission monochromator to minimize the contribution of vesicle-induced scatter to the fluorescence signal. Fluorescence spectra were corrected for Raleigh scatter and background fluorescence by subtraction of the spectra of the appropriate control samples that did not contain protein. In addition, all samples were corrected for the contribution of tyrosine fluorescence emission to the sample signal by subtraction of the fluorescence emission spectrum for Trp^- colicin E1 channel peptide.

Furthermore, for each spectrum, the λ_{em}max was determined by identifying the emission wavelength at which the slope of the first derivative of the spectrum was zero. The REES was the difference between the λ_{em}max for the spectra obtained at excitation wavelengths of 287.5 and 297.5 nm.

2.6. Synthesis of Lys-Trp-Lys

The synthetic tripeptide, Lys-Trp-Lys, was prepared and purified by RP-HPLC by Queen's University Peptide Synthesis Lab and was shown to be greater than 99% pure by mass spectrometry (Queen's University, Kingston, ON). The molar extinction coefficient for the peptide, $\varepsilon_{280\ nm}$=5690 $l \cdot mol^{-1}\ cm^{-1}$, calculated according to the method of Gill and von Hipple [33], was used to determine the peptide concentration.

2.7. Spectroscopic measurements of Lys-Trp-Lys

Samples were prepared in quartz cuvettes (0.5 cm path length), and contained either 62.6 μM Lys-Trp-Lys or 62.6 μM Lys-Trp-Lys and 124 μM DMPS LUVs buffered in 20 mM Tris–acetate, pH 7.0. The phase transition temperature (T_m) of the DMPS LUVs was determined by measuring the λ_{em}max of membrane-associated samples over a range of temperatures from 17 to 55 °C with the excitation wavelength at 287.5 nm. A 299-nm cutoff filter was used (Oriel) to minimize the contribution of LUV-induced scatter to the signal and the fluorescence emission spectra were collected by scanning from 300 to 425 nm.

The effect of red-edge excitation on the λ_{em}max of Lys-Trp-Lys in the presence and absence of DMPS LUVs was examined at temperatures ranging from below to above the T_m by comparing the λ_{em}max for spectra obtained using excitation light of wavelength 287.5 and 297.5 nm (4-nm excitation and 6-nm emission bandpasses).

3. Results and discussion

3.1. Sites of Trp residues in the various single Trp channel peptides

A simple illustration of the location of the three naturally occurring Trp residues (W-424, -460, and -495) and the positions where Trp residues have been substituted for Phe (F-404W, -413W, -431W, -443W, and -484W), and Tyr (Y-367W, -478W, and -507W) or Ile (I-499W) is shown in Fig. 2. Tyr-367 is located at the N-terminus of helix 2 and is largely buried at the interface between helices 8, 9, and 10 in the X-ray structure [3]. Phe-404 is located in the loop region between helices 3 and 4 and is nearly fully exposed [29]; Phe-413 is located in the middle of helix 4 and appears to be partially exposed to solvent and relatively close to Trp-495. Trp-424 is largely buried in the middle of helix 5_a, a small polar helix. Phe-431 is located in the middle of the small helix 5_b, a very flexible region of the channel peptide, and is mostly buried and inaccessible to the aqueous solvent. Phe-443 is located in the extended loop structure between helices 5_b and 6, and is close to residue Lys-470, which is a candidate as a source of the internal quenching seen in the F-443W single Trp mutant [34]; the F-443W residue is also highly exposed to the aqueous solvent [29]. Trp-460 is located in a moderately polar region within the channel peptide, near the N-terminus of helix 7 (Fig. 2). Tyr-478 is positioned in a nonpolar microdomain that is virtually solvent inaccessible and is surrounded by residues Leu-428, Leu-442, Phe-443, Tyr-445, Val-447, and Leu-467. Phe-484 is located in the middle of helix 8 and is well sequestered from solvent but may become exposed by any movement of helices 1 or 2. Trp-495 is situated at the N-terminus of helix 9 and is only slightly exposed to the aqueous solvent. Ile-499 packs against Trp-495 and is positioned in close proximity to Trp-460 and Phe-393. The distal end of the Ile-499 side chain is encircled about by Phe-413 that would likely render this residue largely solvent inaccessible although no acrylamide quenching data exists for the I-499W mutant. Tyr-507 is located in a nonpolar environment provided by Ile-383, Ala-389, Leu-467, Val-479, Leu-483, and Ile-503. Furthermore, Tyr-478, Phe-484, Trp-495, Ile-499, and Tyr-507 are located within the hydrophobic domain of the channel peptide, a nonpolar segment of the peptide consisting of a stretch of 35 amino acid residues; consequently, these Trp residues substituted

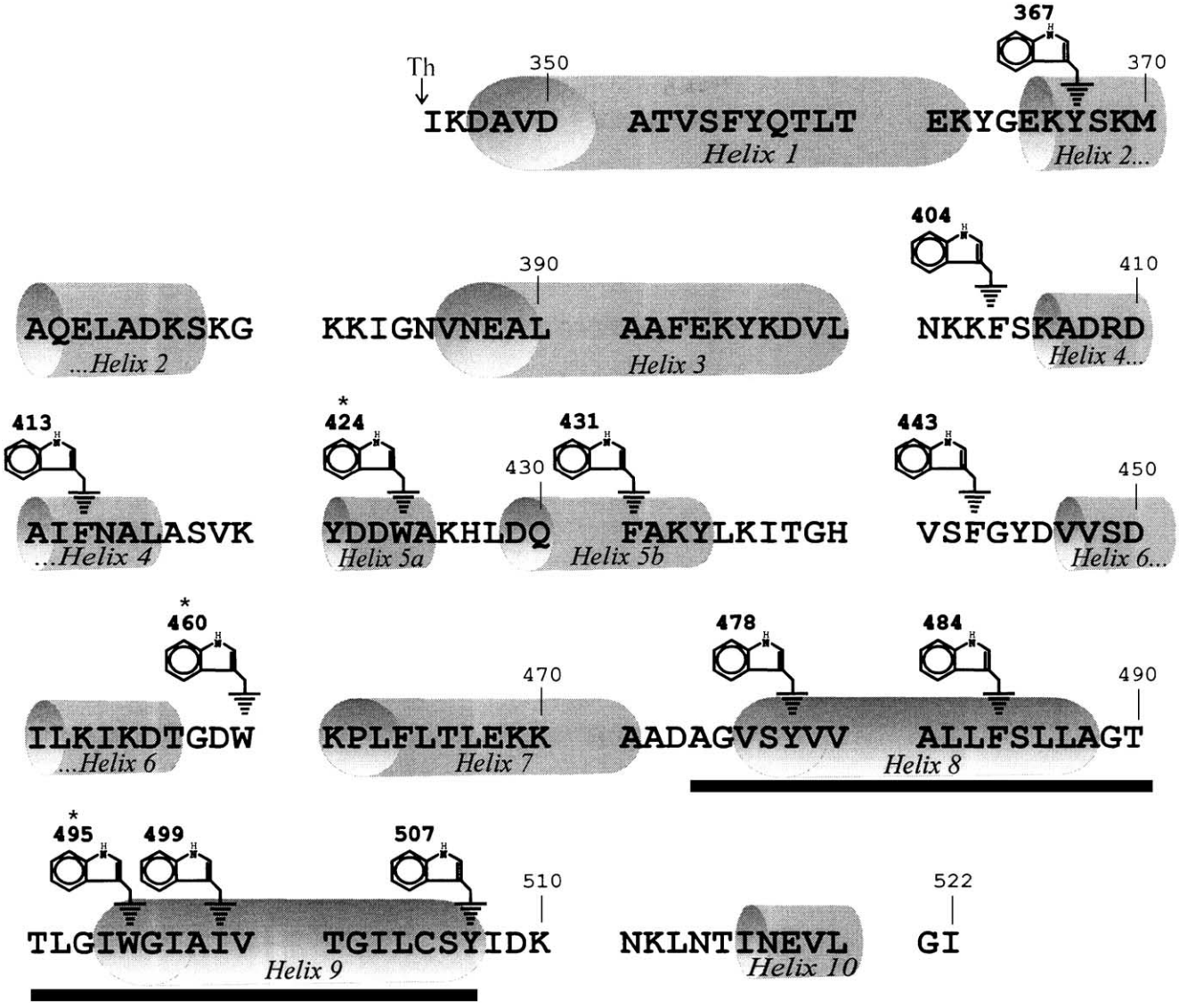

Fig. 2. Primary sequence of the thermolytic colicin E1 channel peptide. Residue numbering corresponds to the numbering of whole colicin E1 [22]. The locations of the α-helices assigned from the crystal structure of the P190 peptide [3] are indicated and the hydrophobic α-helical domain (A-474 to I-508) is underscored. The three naturally occurring Trp residues are identified with an asterisk above the corresponding residue number and the sites where a Trp residue has been substituted into the peptide by site-directed mutagenesis to generate single Trp mutants [29] are indicated by indole rings.

within this protein segment (including Trp-495, a naturally occurring residue) should report peptide structural changes involving the purported membrane anchor domain.

3.2. Red-edge excitation as a probe of the local environment of tryptophan residues in the soluble colicin E1 channel peptide

The degree of REES exhibited by WT and each of the 12 single Trp mutants of colicin E1 channel peptide is summarized in Table 1. The red-edge effect was observed in most but not all of the soluble peptides, indicating that in the low pH-induced insertion-competent state of the soluble channel peptide, most of the single Trp residues are located in a somewhat rigid, solvent-restricted environment and are partially buried within the soluble protein structure [22]. This observation is consistent with previous findings based on anisotropy decay measurements that indicated that the peptide is a very rigid and well-packed globular protein [35].

In contrast to the data for the soluble channel peptide, REES was not observed for either NATA or a 9:1 (mol/mol, identical to that found within most of the single Trp mutant channel peptides) mixture of NAYA/NATA in solution (Fig. 3A). NATA serves as a soluble Trp analogue with peptide bond-like substituents, confirming that a Trp that is fully exposed to rapidly relaxing aqueous solvent does not exhibit any REES. Previously, the red-edge effect has been observed for L-Trp in the viscous environments of glycerol and glucose glasses, but not for L-Trp in aqueous solution

Table 1
Summary of red-edge excitation shift and λ_{em}max values observed for wild-type and single Trp mutants of colicin E1 channel peptide

Protein	Red-edge excitation shift (nm)		λ_{em}max (nm)			
	Soluble[a]	Membrane-associated[a]	Soluble[b]		Membrane-associated[b]	
			Blue[c]	Red[c]	Blue[c]	Red[c]
WT	−1.5±2.1	6.0±0.0	324	322.5	325	331
Y-367W	−1.0±0.3	10.5±0.3	319	318	320.5	331
F-404W	1.5±0.6	3.5±0.0	339	340.5	332.5	336
F-413W	7.0±1.1	6.5±2.0	329	336	330.5	337
W-424	4.5±0.9	9.0±1.5	327.5	332	322.5	331.5
F-431W	1.5±1.8	5.5±0.5	334.5	336	328	333.5
F-443W	0±1.2	0.5±0.9	350	350	338	338.5
W-460	2.0±0.3	11.0±0.9	319.5	321.5	320	331
Y-478W	0.0±0.5	8.0±1.4	326.5	326.5	323.5	331.5
F-484W	7.5±0.8	8.0±0.3	324.5	332	323	331
W-495	6.0±0.9	8.0±0.4	325	331	322	330
I-499W	−2.0±0.4	9.0±2.3	326.5	324.5	323	332
Y-507W	2.5±1.0	8.5±0.7	323	325.5	327	335.5

[a] Values shown are the mean of at least three independent measurements. The error is the standard deviation of the mean. Conditions were as described in Fig. 2 (see also Materials and methods).

[b] Values shown are the mean of at least three independent measurements and the error for all the samples is within 1.5%. The λ_{em}max values are shown for at least three experiments.

[c] Blue and Red denote an excitation wavelength of 287.5 and 297.5 nm, respectively.

[36]. In addition, Lakowicz and Keating-Nakamoto [25] reported that the fluorophore 2-(*p*-toluidinyl) naphthalene-6 sulfonic acid (TNS) did not exhibit any red-edge effect in methanol or dioxane, but did show a REES when bound to the proteins apomyoglobin, β-lactoglobulin, β-casein, and serum albumin. More recently, Falls et al. [37] observed a large REES effect for an engineered Trp residue within a synthetic peptide, which included the N-terminal 46 residues of human prothrombin that was bound to phospholipid membranes.

The absence of the red-edge effect for the 9:1 (mol/mol) NAYA/NATA solution indicates that when the Trp chromophore is free in aqueous solution in the presence of Tyr at a molar ratio identical to that found in most of the single Trp channel peptides, no spectroscopic artifacts are observed. Furthermore, these results indicate that the freely rotating and unrestricted indole chromophore does not exhibit any significant shift in its λ_{em}max upon selective red-edge excitation. The fluorescence spectra for the channel peptides were also corrected for any contributions of tyrosine fluorescence using the Trp-deficient mutant channel peptide (Trp^-); however, this correction does not account for Tyr–Trp energy transfer. If a Tyr-deficient mutant colicin E1 channel peptide were prepared by site-directed mutagenesis, the contribution of energy transfer could be assessed. However, the preparation of a Tyr-deficient mutant protein was impractical due to the number of mutations required to replace all nine Tyr residues within the channel peptide. Furthermore, it would also be highly questionable as to the relevance the results of a study using this mutant channel peptide would have to the native single Trp mutants of the colicin E1 channel peptide due to the high probability for structural perturbation. Chemical modification of the Tyr residues was also not attempted for similar reasons.

The Trp residues at positions 367, 443, 478, and 499 did not exhibit any significant REES in the soluble peptide (Table 1), indicating that each of these residues is either completely exposed to rapidly relaxing solvent, or situated within a hydrophobic region of the peptide, where the concentration of polar solvent and/or nearby polar groups is minimal. The ambiguity in assigning the locale for a chromophore reveals an apparent limitation of the red-edge excitation technique, which is that the fluorescence emission maximum value must also be considered in order to assess the location of the Trp residue within a protein. Furthermore, REES data are required for both the soluble and the membrane-bound forms of the peptide in order to compare changes in environment that may occur upon membrane association.

3.3. Surface accessibility of Trp residues in soluble peptide

A surface-accessibility simulation in which the relative exposure of each residue to a sphere of radius 1.4 Å (water

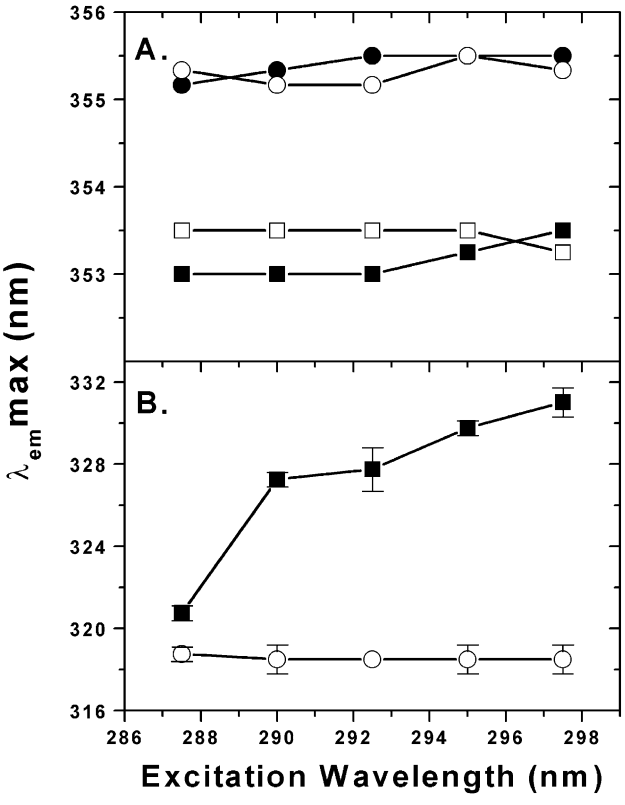

Fig. 3. Dependence of fluorescence emission maximum on excitation wavelength. (A) NATA in the absence (○) and presence (●) of LUVs; NAYA/NATA (9:1, mol/mol) in the absence (□) and presence (■) of LUVs. (B) Y-367W channel peptide in the absence (○) and presence (■) of 60:40 mol/mol DOPC/DOPG LUVs. All samples were in 100 mM NaCl and 10 mM DMG at pH 3.5 with conditions as specified in Materials and methods.

molecule) rolled along the surface of the colicin E1 channel peptide crystal structure is shown in Fig. 4. Y-367 and Y-478 are among the least surface accessible residues in the peptide (P. Elkins, personal communication). Analysis of the crystal structure for the channel peptide (water-soluble state) reveals that Y-367 is mostly buried in the soluble protein near the interface of helices 8, 9, and 10 (C. Stauffacher, unpublished data). In addition, acrylamide-quenching studies indicated that Y367W is only partially exposed to soluble quenchers (k_q=0.86 M^{-1} ns^{-1} at pH 3.5; [29]). Finally, the λ_{em}max for Y-367W is the most blue-shifted of the residues under consideration (320 nm) relative to NATA in buffer (350 nm), indicating a nonpolar environment for this residue within the soluble peptide [29]. This evidence, combined with the absence of a REES, provides a strong argument that Y-367W is situated in a nonpolar environment, which is sequestered from aqueous solvent.

The accessibility of Trp-478 to acrylamide indicated that it is largely buried in the soluble peptide and that it remains quite inaccessible to the solvent upon membrane association [22], in agreement with its blue-shifted λ_{em}max (326 nm) relative to NATA in aqueous solution. As for Y-367, X-ray structural evidence also supports a nonpolar environment for Y-478 that is consistent with the lack of REES in the soluble form of this mutant peptide. Demchenko [28] proposed that for proteins emitting at short wavelengths, the Trp residue(s) are in a hydrophobic environment and the dipole-orientational broadening of the spectra is insufficient to give rise to REES [38].

In contrast, the absence of the red-edge effect for F-443W is a result of the considerable exposure of this residue to bulk aqueous solvent. From the crystal structure, F-443 is located in an extended polar loop region, between helices 5_b and 6, where it is exposed to solvent and also the surface accessibility plot (Fig. 4) indicates that F-443 is very solvent exposed. Acrylamide quenching results (k_q=1.79 M^{-1} ns^{-1} at pH 3.5) corroborate the X-ray data indicating that F-443W is indeed surface-exposed in the soluble peptide. Also, the λ_{em}max for F-443W (338 nm) is the most red-shifted of any of the single Trp residues within the channel peptide [29], supporting a solvent-exposed, polar environment for F-443W. This observation agrees with the proposal by Demchenko [28], who purported that in the case of the very long wavelength-emitting proteins, the Trp residues are exposed to an aqueous environment undergoing much faster solvent relaxation as compared to the fluorescence decay rates ($1/\tau_F$) of those Trp residues [38].

The largest REES values were observed for F-413W, W-424, F-484W, and W-495 soluble proteins (Table 1), which suggest that the microenvironment of these residues is rigid with respect to solvent dipolar reorientation, resulting in fluorescence emission from a nonequilibrium state [39]. Acrylamide quenching studies [29] classified W-424 and F-484W as moderately buried residues, while F-413W and

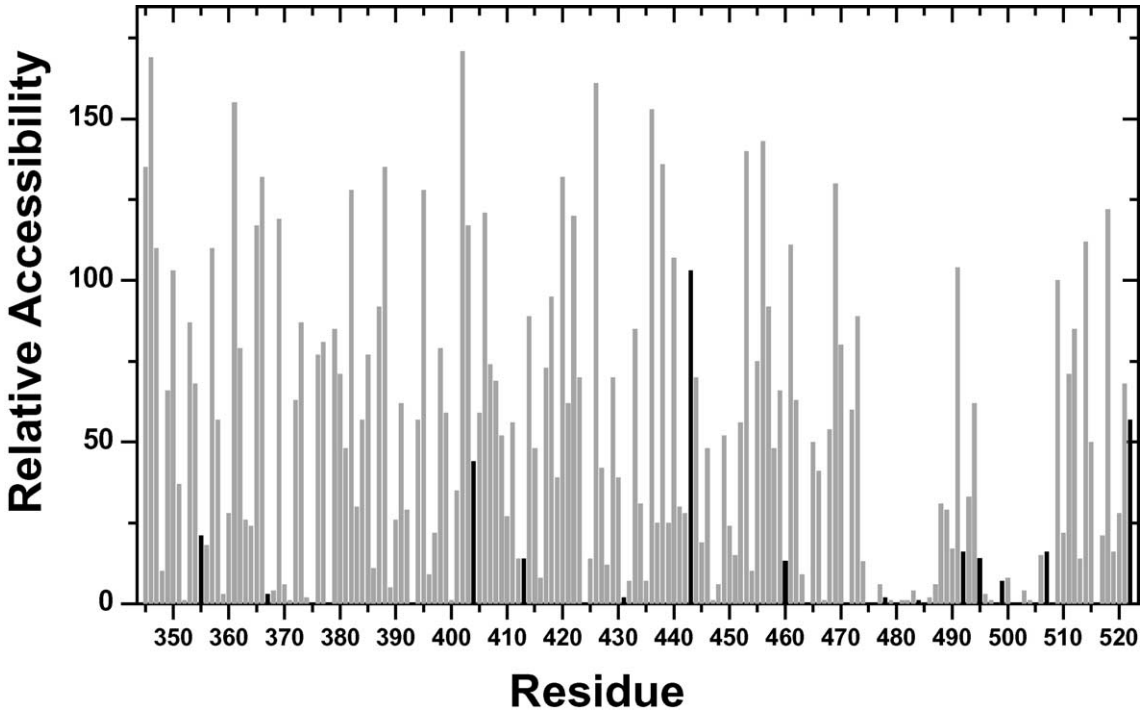

Fig. 4. Surface accessibility of the colicin E1 channel peptide to aqueous solvent. The X-ray structure of the thermolytic colicin E1 channel peptide was subjected to a residue surface-accessibility calculation using a probe of 1.4 Å and software from the CCP4 Suite: Programs for Protein Crystallography (http://www.ccp4.ac.uk/main.html). The black bars indicate those residues where a Trp residue is found (either naturally or by mutagenesis) within the colicin E1 channel peptide.

W-495 were classified as moderately exposed residues. From the crystal structure, W-424 is predominantly buried within helix 5_a, in a location that appears to be only partially solvent accessible. The presence of several potential hydrogen-bonding groups within a 5 Å radius of the indole -NH group of W-424 is the most probable source of the restriction of solvent dipolar reorientation in this region [3].

Phe-484 is positioned in the centre of helix 8, which is located within the hydrophobic anchor domain. From the crystal structure, F-484 would be expected to be partially solvent exposed (C. Stauffacher, personal communication). Several potential hydrogen-bonding groups originating from Y-356, A-481, S-485, and A-488 are situated within 5 Å of the side chain of F-484. Any water molecules in the immediate environment of F-484 might be subject to interaction with these residues, resulting in solvent restriction and may account for the large REES observed for the F-484W mutant.

Phe-413 is located in the middle of helix 4 and appears to be partially exposed to solvent in the X-ray structure [3] and is relatively close to Trp-495. Acrylamide quenching data indicate that F-413W is moderately exposed to the aqueous solvent (k_q=0.90 M^{-1} ns^{-1} at pH 3.5; [29]).

Moreover, the λ_{em}max for F-413W was 327 nm at acidic pH that provides additional support to Trp-413 being partially exposed to solvent in the soluble peptide [29]. Again, the surface accessibility data (Fig. 4) indicate partial exposure of Phe-413.

W-495, located at the N-terminus of helix 9, is also located within the hydrophobic anchor domain. Based on the crystal structure and surface-accessibility simulation data (Fig. 4), W-495 would be expected to be moderately solvent-exposed. The decreased concentration of solvent molecules in the region surrounding W-495 increases the probability that the surrounding solvent molecules in the vicinity of this naturally occurring Trp residue are involved in dipolar, electrostatic, and/or hydrogen-bonding interactions. As a result of these interactions, Trp-495 would likely be at least partially restricted in its mobility, resulting in a significant REES effect.

The residues that exhibited a very modest (<3 nm) REES were F-404W, F-431W, W-460, and Y-507W, indicating that these residues exist in a slightly restricted environment (Table 1). F-404 is predicted to be mostly solvent exposed, in the loop region between helices 3 and 4 [3]. This is also substantiated by the surface accessibility plot of the channel peptide (Fig. 4) and by the fluorescence λ_{em}maximum of 334 nm [29]. Acrylamide quenching data identified the Trp residue in the F-404W mutant peptide as moderately exposed (k_q=1.36 M^{-1} ns^{-1} at pH 3.5, [29]). Due to the modest REES effect observed for F-404W, the solvent surrounding the Trp must be involved in a limited number of dipolar interactions, which slow the reorientation of solvent molecules that occurs following excitation. Y-507W is predicted to be only partly solvent accessible and was classified as moderately buried at acidic pH in aqueous solution (k_q=0.29 M^{-1} ns^{-1}; [29]; Fig. 4). The λ_{em}max value for the Y-507W channel peptide is 323 nm, which also indicates a partially buried environment for this Trp residue. The extent of solvent exposure and the nature of the surrounding side chains would be expected to result in partial restriction of surrounding solvent molecules and slow solvent relaxation times, relative to the fluorophore lifetime. Similarly, W-460 is located at the N-terminus of helix 7, in a moderately solvent-exposed, polar region ([29]; Fig. 4) and its REES would be expected to be similar to that observed for Y-507W.

Phe-431 is located in a flexible region of the peptide, in the middle of helix 5_b, where it is mostly inaccessible to solvent. The small red-edge effect that is observed for F-431W is most likely a result of the interactions of a limited number of solvent molecules with nearby polar residues, and with the indole -NH group of the Trp residue. The λ_{em}max value for F-431W (335 nm) suggests, however, that the residue is situated in a relatively polar environment [29], which may indicate that it interacts with polar groups within the protein structure.

In summary, the REES values observed were grouped into three classifications, (i) Trp residues that did not exhibit REES as a result of their location in a solvent-exposed (F-443W) or hydrophobic (Y-367W, Y-478W, and I-499W) environment; (ii) Trp residues that exhibited a modest REES of up to 2.5 nm as a result of limited solvent restriction or interaction with polar groups on or near the surface of the protein (F-404W, F-431W, W-460, and Y-507W); and (iii) Trp residues that exhibited a large (>4 nm) REES as a result of more restrictive dipolar interactions (F-413W, W-424, F-484W, and W-495) (Table 2).

No significant REES effect was observed for the WT colicin E1 channel peptide. This REES is difficult to interpret without considering the component spectra of each of the Trp residues, and the possible contribution(s) of energy transfer that could occur between the three native Trp residues and/or from Tyr to Trp residues. Two of the single Trp mutants derived from native Trp residues, W-424 and W-495, showed a large REES effect, while the third, W-460, exhibited a small REES (Table 1). This may indicate that the average Trp environment in WT channel peptide is

Table 2
Classification of colicin E1 channel peptides according to the magnitude of ΔREES upon membrane binding

ΔREES[a] classification	ΔREES observed	Channel peptides
Small	0≤ΔREES≤3 nm	F-404W, F-413W, F-443W, F-484W, W-495
Intermediate	3<ΔREES≤7 nm	W-424, F-431W, Y-507W
Large	7<ΔREES≤12 nm	WT, Y-367W, W-460, Y-478W, I-499W

[a] ΔREES represents the difference between REES for the membrane-bound peptide ($REES_{mem}$) and the REES for the soluble peptide ($REES_{sol}$), i.e. $\Delta REES = REES_{mem} - REES_{sol}$ (see Table 1 for the REES values).

most like that of W-460; however, it is more likely that energy transfer contributions and internal quenching mechanisms are active, confounding the results [34].

Overall, the environment predicted for each single Trp residue from the magnitude of the REES observed was in good agreement with previous studies of the Trp environments. The use of red-edge excitation to probe the local environment of other engineered single Trp proteins appears to be a feasible method to probe the solvent dynamics and/or extent of interaction with polar groups within selected regions of a protein. Thus, information derived from REES analysis can shed further light on the relative mobility and interactions with the polar solvent water and/or polar groups on the surface of a protein.

3.4. Effect of red-edge excitation of tryptophan localized to different regions of a model membrane bilayer

In order to elucidate the degree of REES expected for a tryptophan residue located in different regions of a membrane bilayer, a model system composed of a synthetic tripeptide, Lys-Trp-Lys, and DMPS LUVs was employed. The sequence for the tripeptide was chosen because the indole side chain of the tryptophan residue provides a source of intrinsic fluorescence, while the positively charged lysine residues permit the electrostatic interaction of the peptide with the negatively charged phospholipid headgroups of membrane bilayers.

The interaction of Lys-Trp-Lys with DMPS membranes has previously been characterized using fluorescence spectroscopic techniques [40]. Specifically, a temperature-dependence of the λ_{em}max for the Trp residue of Lys-Trp-Lys associated with DMPS LUVs was observed, which corresponded to the phase transition temperature (T_m=31 and 39 °C at pH 7 and 5, respectively) of the lipid system [40].

From previous work on the Lys-Trp-Lys system, Yamashita et al. [40] concluded that at temperatures below the T_m, the indole side chain of Lys-Trp-Lys is located in close proximity to the phospholipid headgroups, but is not inserted within the hydrocarbon portion of the membrane, likely due to the tight packing of the fatty acyl chains in the gel phase of the phospholipid membrane. At temperatures above the T_m, however, the fluid phase results in looser packing of the lipid acyl chains. As a consequence of the loose packing, the Trp residue can enter the bilayer, resulting in the intercalation of the indole side chain within the acyl chain region of the bilayer, rather than at the interface as for the gel phase.

The red-edge excitation behaviour of Lys-Trp-Lys within DMPS LUVs was examined at temperatures ranging from below to above the T_m (T_m=29 °C as determined by fluorescence polarization measurements with diphenylhexatriene as the fluorescence reporter; data not shown) to elucidate the degree of REES expected for a Trp residue located in the interfacial region of the bilayer, compared to that expected for a Trp residue buried deep within the hydrophobic core of the membrane.

The temperature-dependence of the REES observed for Lys-Trp-Lys in the absence and presence of DMPS LUVs is summarized in Fig. 5. In the absence of LUVs, the temperature-dependence of the red-edge effect for the model peptide in aqueous solution was negligible. However, the red-edge effect for Lys-Trp-Lys associated with DMPS LUVs was dependent upon the temperature. At temperatures well below the T_m, the REES was very not significant (0.5 nm), and was similar to that observed for the peptide in solution without LUVs, which indicates that the Trp is almost completely exposed to bulk solvent. Yamashita et al. [40] indicated that at temperatures below the T_m, the Trp residue of Lys-Trp-Lys is located near the bulk water–phospholipid headgroup interface of the membrane. Considering the small REES observed, it would appear that the Trp is indeed located at the phospholipid–solvent interface, with the indole side chain projected away from or loosely associated with the membrane surface. The tightly packed phospholipid acyl chains of the gel state bilayer prevent the indole side chain from penetrating the membrane surface.

As the T_m temperature was approached, the REES values started to increase as the Trp side chain began to penetrate the hydrocarbon matrix of the membrane (Fig. 5). This observation is consistent with the observed blue shift in the λ_{em}max value of Lys-Trp-Lys [40], which indicates that at the T_m, the Trp residue is partially buried within the bilayer, but is not as deeply entrenched in the bilayer hydrocarbon milieu as at temperatures that are above the T_m. The Trp residue must, therefore, be largely exposed to bulk solvent at temperatures that are several degrees higher than the T_m where the bilayer is in a highly fluid state.

A model for the insertion of the Trp residue of Lys-Trp-Lys into DMPS LUVs as a function of temperature is presented in Fig. 6. The location of the indole side chain

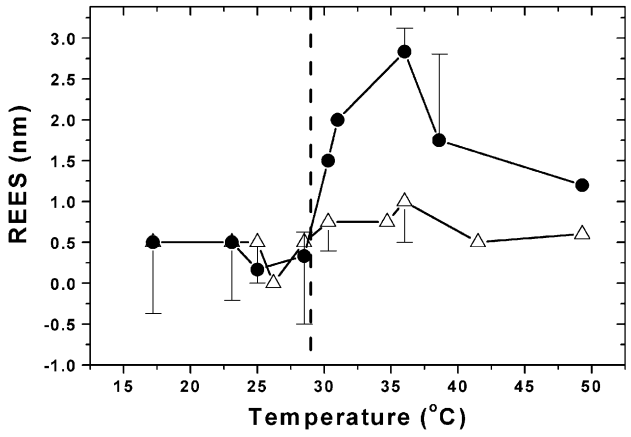

Fig. 5. Temperature dependence of red-edge excitation shift for Lys-Trp-Lys in the absence (△) and presence (●) of DMPS LUVs. The phase transition temperature, T_m, for DMPS LUVs is identified by the vertical dashed line. Samples were prepared in 20 mM TRIS-acetate, pH 7.0 and were analyzed as described in Materials and methods.

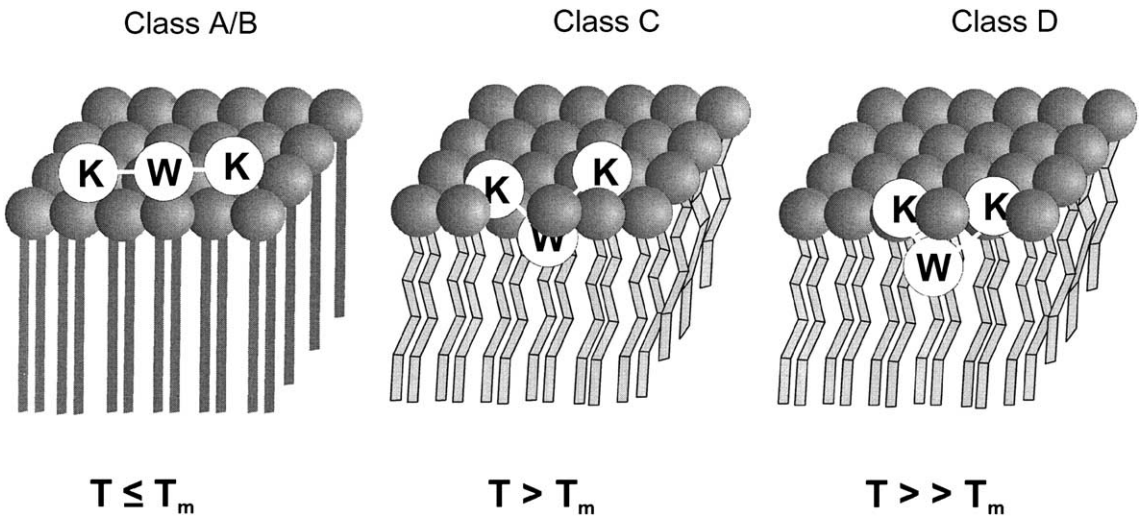

Fig. 6. Model for the red-edge excitation behaviour of Lys-Trp-Lys in association with DMPS LUVs at various temperatures. Class A/B Trp residues are fully exposed to bulk aqueous solvent (Class A), or only slightly embedded within the bilayer (Class B); both classes of residues do not exhibit a significant red-edge effect. A moderate to large red-edge effect is observed for class C Trp residues, which are embedded within the interfacial region of the bilayer. A significant REES is not observed for Class D Trp residues, which are located within the hydrophobic core of the bilayer. The following symbols are used: T, temperature and T_m, phase transition temperature.

of the Trp residue at each stage of the insertion process serves as a model for a class of Trp that might be found in a peptide interacting with a membrane bilayer. The surface-associated Trp (Class A) is largely exposed to bulk aqueous solvent with minimal solvent restriction and, consequently, exhibits little or no red-edge effect ($\tau_S\tau_F$). The Trp residue, which is slightly embedded within the bilayer (Class B), experiences a slightly less polar environment than Class A Trp residues, but residues and the degree of restriction of polar (water) solvent near the fluorophore is marginal. Consequently, class B Trp residues show small REES effects. The largest REES is expected for Class C Trp residues, which are situated at the phospholipid headgroup–acyl chain interface where the interaction of the phospholipid polar headgroups with solvent dipoles surrounding or associated with the Trp residue prevent solvent relaxation from occurring within the excited state lifetime ($\tau_S \gg \tau_F$). The final class of Trp residues, Class D, is found more deeply embedded within the hydrophobic region of the membrane, where the reduced water concentration and diminished interaction with the polar components of the phospholipid headgroups, combined with the increased kinetic energy at higher temperatures, reduces the magnitude of the red-edge effect. This situation is likely similar to that described by Demchenko [38] for relatively polar fluorophores in a nonpolar solvent.

3.5. Red-edge excitation as a probe of the membrane topology of colicin E1 channel peptide

The magnitude of the REES observed for the membrane-associated single Trp mutant channel peptides provides information regarding the nature of the interaction of the indole side chain at various sites throughout the channel peptide sequence with the polar phospholipid headgroups and/or with restricted water molecules. Considering the results of red-edge excitation studies on model systems and the degree of solvent restriction expected in different regions of the bilayer, the relative position of the Trp residue within the bilayer could be determined. Previously, red-edge excitation experiments have been performed on membrane-associated proteins containing one or more Trp residues [37,41–43] to characterize the environment of the Trp residues. These studies have not, however, exploited the ability to generate mutant proteins containing single Trp residues at sites of interest. This would appear, therefore, to be the first attempt at using red-edge excitation as a site-specific probe of the membrane topology of a membrane protein.

With the exception of F-413W, F-443W, and F-484W, all of the peptides investigated exhibited a significantly larger REES (Table 1) for the membrane-associated peptide than for the soluble peptide. Zhang and Cramer [13] demonstrated the presence of a limited number of protease accessible sites on the membrane-associated channel peptide, indicating, in general, that the peptide is closely appressed to the bilayer surface. The tight interaction of the channel peptide with the membrane surface would likely result in a reduced number of solvent molecules available for interaction with the peptide, and also an increased interaction of the indole side chain with the polar substituents of the phospholipid headgroups, thus resulting in a more solvent-restricted environment for the Trp residues within the channel peptides in the membrane-bound conformation as compared with the soluble state. Perhaps, those Trp residues that show significant REES are located at those solvent-restricted sites with the colicin channel peptide.

The red-edge effect on the λ_{em}max of Y-367W in the soluble and membrane-associated states is presented in Fig.

3B. The red-edge effect is absent for Y-367W channel peptide in solution, probably due to the location of Trp-367 at the hydrophobic, solvent-excluded interface of helices 8, 9, and 10. Upon interaction with model membrane vesicles, however, a large REES of 10.3±0.4 nm was observed, indicating that the residue is situated in an environment that offers considerable restriction of solvent mobility near the membrane–bilayer interface.

Based on the REES data obtained for the model system, it was proposed that the largest REES values would be observed for Trp residues located within the interfacial region of the bilayer (Fig. 5). Other model studies have resulted in similar hypotheses. The red-edge excitation behaviour of several fluorescent probes incorporated within membrane bilayers has been studied. The NBD group of NBD-PE incorporated into DOPC vesicles exhibited a 10 nm REES [44]. Furthermore, an NBD-labeled peptide derived from apolipoprotein exhibited an REES in its emission maximum, consistent with the insertion of the probe into the motionally restricted, polar environment of the bilayer interface [45]. In contrast, the fluorescent probes 1-anilinonaphthalene-8-sulfonic acid (ANS) and TNS were not subject to the red-edge effect [46]. Both ANS and TNS would be expected to approach the headgroups of phospholipid bilayers via the aqueous phase, due to the charge on these probes at neutral pH. As a result, the probes are likely situated in the aqueous phase adjacent to the phospholipid headgroup [44], an environment in which solvent restriction is minimal and rapid solvent relaxation can occur. In contrast, the NBD moiety of NBD-PE is fixed at the membrane interface, a region that limits the rate of solvent relaxation around the NBD chromophore [44].

The representation of the bilayer interface as a distinct demarcation is not very realistic considering that King and White [47] have shown that a gradient of solvent water exists throughout the membrane. Moreover, a molecular dynamics simulation of the gramicidin channel within a DMPC phospholipid bilayer [48] indicates that the bilayer interface is, indeed, not a distinct plane, as the transition from polar headgroups to nonpolar acyl chains occurs through a region that is at least 12 Å deep. The solid-state NMR properties of the gramicidin channel [48] are in agreement with the molecular dynamics simulation. Based on the simulation, the interfacial region of the bilayer contains solvent water, glycerol backbone, and phospholipid headgroups, and extends from a depth of 9–21 Å within the bilayer, with the ester carbonyl groups situated at a depth of 12–14 Å [48]. The restricted solvent mobility around Trp residues located within the interfacial region of the membrane is largely a result of hydrogen-bonding interactions between the indole side chain of Trp and solvent water molecules that are tethered to the polar headgroups of the phospholipids. Bechinger and Seelig [49] estimated that each polar headgroup is bound to 20 solvent water molecules, a major contribution to solvent restriction in the membrane interfacial region.

The large REES observed for the membrane-bound Y-367W mutant channel peptide likely indicates that Y-367W is localized in the interfacial region of the membrane. An interfacial position for Y-367W is supported by the susceptibility of S-368 of membrane-bound WT colicin E1 channel peptide to chymotrypsin [13]. In a model of the membrane topology of the colicin E1 channel peptide proposed by Palmer and Merrill [15], Y-367W was positioned in a moderately buried location, 8.0 Å from the C-2 carbon of the phospholipid fatty acyl chain. This location is within the interfacial region of the bilayer defined by Woolf and Roux [48].

Since a significant red-edge effect exists within the soluble channel peptide, and therefore a background "noise" level of REES is present, it is paramount for the interpretation of the red-edge effect for the membrane-bound channel structure to correct for the REES effect observed within the soluble protein. The data shown in Fig 7 represent the difference between the REES effect in the membrane-bound state and that seen in the soluble state ($REES_{mem}-REES_{sol}=\Delta REES$). Applying the criterion for the REES effect as based on our Lys-Trp-Lys model that for the polar Trp chromophore in a membrane system, the Trp residue must be partially buried within the bilayer and interacts with solvent and/or polar substituents in the vicinity of the phospholipid headgroup in order to produce a significant red-edge effect. Therefore, the data shown in Fig 7 indicate that Trp located at positions 367, 460, 478, 499, and 507 are positioned at the membrane bilayer–solvent interface. This implicates three regions within the membrane-bound channel peptide as interfacial and that may be appressed to the liposome surface, which could be a consequence of the orientation of certain faces of helices lying on the membrane surface bathing the corresponding resi-

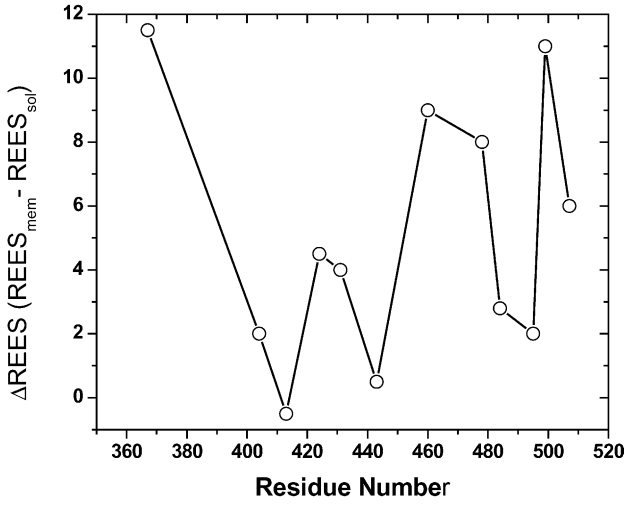

Fig. 7. The ΔREES for the membrane-associated colicin E1 channel peptide. The parameter ΔREES was defined as the REES (membrane-bound state)−REES (soluble state). The REES values were those shown in Table 1 and were determined as described in Materials and Methods.

dues within the acyl chain portion of the bilayer. These regions are: (1) 355–413, (2) 443–484, and (3) 495–507.

Interestingly, these data correlate well with our previous data on the bilayer depths of these Trp residues as determined by depth-dependent fluorescence quenching [15] and acrylamide quenching of Trp fluorescence. In those studies, it was found that the N-terminus (Trp-355 and -367) was located further away from the bilayer center than Trp-393, -404, -413, -424, -431, and -443. Trp-466 and -507 were also located at a distance from the bilayer center that would be expected to correspond to the membrane headgroup interfacial region and, hence, the general topological pattern for the channel peptide bound to the membrane in the absence of a potential is similar as ascertained from the two different approaches. Furthermore, a more recent study from our laboratory showed that upon membrane association, Trp-67, -460, and -507 exhibited red-shifted fluorescence emission maxima as contrasted with the corresponding values in the soluble channel peptide, incidentally where there is little or no REES observed because the Trp residues within the soluble protein structure are located in nonpolar environments [22]. This is indicative of the localization of these Trp residues at similar positions at the headgroup–acyl chain interface. However, Trp-499 showed a slight blue-shift in its fluorescence emission maximum, which may be a consequence of the fine details of the membrane-bound channel peptide structure that are not presently available.

Given the apparent preference of Trp residues for interfacial positions, one must consider whether the insertion of Trp residues at sites of interest throughout the peptide causes a distortion of the channel peptide's membrane topology to allow for an interfacial location for the peptide segment where the Trp was substituted [50]. While this remains a possibility, several factors suggest that the insertion of a Trp does not force a large movement to the interfacial region, including the noteworthy observation that engineered single Trp mutant channel peptides show normal channel activity and gating; however, small shifts in topology may occur.

Other aromatic residues are also frequently found at the bilayer interface [50]. With the exception of I-499W, the single Trp mutants were generated by inducing conservative substitutions of Trp for Tyr or Phe, aromatic residues that would also normally prefer an interfacial location within the bilayer. If an induced interfacial location resulted from the substitution of a nonaromatic amino acid with Trp, it would most likely be for the mutant I-499W, which exhibited a large REES. An interfacial location for the hydrophobic Ile side chain would be less favorable than for Trp, so it is possible that the Trp residue would distort the membrane conformation of the channel peptide to attain an interfacial position. However, each of the mutant channel peptides was functional with respect to cytotoxicity and in vitro channel-forming activity [29,30] at levels comparable to WT channel peptide, and the secondary structural was unaltered as a result of the mutations [29]. Therefore, it is not likely that the substitution of a Trp at position 499 resulted in a large alteration of the membrane topology of the channel peptide. However, a complication arises from the earlier finding that the membrane-associated colicin E1 channel peptide assumes a dynamic topology in which a large degree of movement within the confines of the membrane occurs, especially for the hydrophobic hairpin region [51,52]. In contrast with the movement of entire helices within the bilayer, the effect of a slight preference of one residue (I-499W) for an interfacial location on membrane topology would not be significant; however, the position of a *trans*-membrane helix could also be shifted as a result of the peptide's movement.

In summary, the REES data concerning the membrane-bound topology of the colicin E1 channel peptide is consistent with the previous models suggested for the closed state of the channel [11,13,15,16,22,51–54]. Important components of the models for the closed channel state include a monomeric species that features the partial immersion of helices 1 and 2 into the bilayer and the flickering of the hydrophobic domain (helices 8 and 9) between states 1 and 2 as suggested by Kienker et al. [51] except that state 2 is not fully *trans*-membrane. Depth-dependent quenching data suggest that state 2 is the preferred orientation and is the most heavily populated state for the closed channel structure [53]. The imposition of a membrane potential induces the formation of a mature, open channel by the translocation of the gating peptide [17,18,55] comprised of helices 5–7 from the soluble structure. However, recent data employing engineered epitopes suggest that colicin Ia is capable of translocating a much larger segment of hydrophilic peptide than previously believed possible and that the C-terminal 85 residues (residues 542–626 of Ia) functions as a protein translocator [56]. It now seems likely that the gating peptide is part of a larger protein segment that moves across the membrane bilayer in response to an imposed membrane potential [51,56]. However, considering that each channel entity is composed of a single colicin polypeptide, it seems reasonable to suggest that the channel makes use of nearly all of the polypeptide sequence [22,51–56]. This channel (helix bundle) structure undoubtedly must involve sufficient polypeptide length to form an ion channel with a lumen of the physical dimensions as shown previously [57] with a 7 Å pore [58]. Presently, the model for the closed state of the colicin channel provides a working hypothesis that can be subjected to the rigors of membrane biochemical/biophysical experiments.

In conclusion, the site-specific approach described in this work, which involved mapping the membrane topology of colicin E1 using the REES method, should prove helpful in the investigation of other membrane proteins, particularly for identifying regions of the peptide that reside in the interfacial region of the bilayer. However, a note of caution is necessary concerning the potential ambiguity in the interpretation of REES data. It is not possible to differentiate between the

situation for a Trp residue located within a restricted site in the soluble peptide as contrasted with a Trp residue found at a deep location within the bilayer interface. It is therefore necessary to measure the REES for both the soluble and membrane-bound peptides and to compare the REES changes in both states of the protein ($\Delta REES = REES_{mem} - REES_{sol}$; see Fig. 7). Additionally, with respect to the REES measurements of membrane-associated peptides, it is not possible to resolve the *cis* or *trans* location of the Trp residue; however, it may be feasible to discriminate between Trp residues that are located on the *cis* or *trans* side of the membrane bilayer by employing LUVs that are loaded with a high viscosity solute.

Acknowledgements

This work was supported by the Natural Sciences and Engineering Research Council of Canada (ARM).

We thank Professor Patrick Callis for helpful suggestions and critical reading of the manuscript.

References

[1] M. Wiener, D. Freymann, P. Ghosh, R.M. Stroud, Nature 385 (1997) 461–464.
[2] M.W. Parker, J.P. Postma, F. Pattus, A.D. Tucker, D. Tsernoglou, J. Mol. Biol. 224 (1996) 639–657.
[3] P. Elkins, A. Bunker, W.A. Cramer, C.V. Stauffacher, Structure 5 (1997) 443–458.
[4] I.R. Vetter, M.W. Parker, A.D. Tucker, J.H. Lakey, F. Pattus, D. Tsernoglou, Structure 6 (1998) 863–874.
[5] K.R. Brunden, Y. Uratani, W.A. Cramer, J. Biol. Chem. 259 (1984) 7682–7687.
[6] D.R. DiMasi, J.C. White, C.A. Schnaitman, C. Bradbeer, J. Bacteriol. 115 (1973) 506–513.
[7] J. Dankert, Y. Uratani, C. Grabau, W.A. Cramer, W.A. Hermodson, J. Biol. Chem. 257 (1982) 3857–3863.
[8] J.M. Gould, W.A. Cramer, J. Biol. Chem. 252 (1977) 5491–5497.
[9] M.B. Cleveland, S. Slatin, A. Finkelstein, C. Levinthal, Proc. Natl. Acad. Sci. U. S. A. 80 (1983) 8706–8710.
[10] W.A. Cramer, J.R. Dankert, Y. Uratani, Biochim. Biophys. Acta 737 (1983) 173–193.
[11] W.A. Cramer, J.B. Heymann, S.L. Schendel, B.N. Deriy, F.S. Cohen, P.A. Elkins, C.V. Stauffacher, Annu. Rev. Biomol. Struct. 24 (1995) 611–641.
[12] J.H. Lakey, F.G. van der Goot, F. Pattus, Toxicology 87 (1994) 85–108.
[13] Y.-L. Zhang, W.A. Cramer, Protein Sci. 1 (1992) 1666–1676.
[14] H.Y. Song, F.S. Cohen, W.A. Cramer, J. Bacteriol. 173 (1991) 2927–2934.
[15] L.R. Palmer, A.R. Merrill, J. Biol. Chem. 269 (1994) 4187–4193.
[16] Y.-K. Shin, C. Levinthal, W.L. Hubbell, Science 259 (1993) 960–963.
[17] A.R. Merrill, W.A. Cramer, Biochemistry 29 (1990) 8529–8534.
[18] S.L. Slatin, X.-Q. Qui, K.S. Jakes, A. Finkelstein, Nature 371 (1994) 158–161.
[19] K.B. Strawbridge, L.R. Palmer, A.R. Merrill, F.R. Hallett, Biophys. J. 68 (1995) 131–136.
[20] S.D. Zakharov, M. Lindeberg, Y. Griko, Z. Salamon, G. Tollin, F.G. Prendergast, W.A. Cramer, Proc. Natl. Acad. Sci. U. S. A. 95 (1998) 4282–4287.
[21] Y. Kim, K. Valentine, S.J. Opella, S.L. Schendel, W.A. Cramer, Protein Sci. 7 (1998) 342–348.
[22] M.C. Tory, A.R. Merrill, J. Biol. Chem. 274 (1999) 24539–24549.
[23] A. Nardi, S.L. Slatin, D. Baty, D. Duche, J. Mol. Biol. 307 (2001) 1293–1303.
[24] S.D. Zakharov, M. Lindeberg, W.A. Cramer, Biochemistry 38 (1999) 11325–11332.
[25] J.R. Lakowicz, S. Keating-Nakamoto, Biochemistry 23 (1984) 3013–3021.
[26] A.N. Rubinov, V.I. Tomin, Opt. Spectrosc. 29 (1970) 578–580.
[27] R.B. Macgregor, G. Weber, Ann. N. Y. Acad. Sci. 366 (1981) 140–154.
[28] A.P. Demchenko, Eur. Biophys. J. 16 (1988) 121–129.
[29] A.R. Merrill, L.R. Palmer, A.G. Szabo, Biochemistry 32 (1993) 6974–6981.
[30] B.A. Steer, A.R. Merrill, Biochemistry 33 (1994) 1108–1115.
[31] G.R. Bartlett, J. Biol. Chem. 234 (1958) 466–468.
[32] B.N. Ames, D.T. Dubin, J. Biol. Chem. 235 (1960) 769–772.
[33] S.C. Gill, P.H. von Hippel, Anal. Biochem. 182 (1989) 319–326.
[34] B.A. Steer, A.R. Merrill, Biochemistry 34 (1995) 7225–7233.
[35] A.R. Merrill, B.A. Steer, G.A. Prentice, M.J. Weller, A.G. Szabo, Biochemistry 36 (1997) 6874–6884.
[36] A.P. Demchenko, A.S. Ladokhin, Eur. Biophys. J. 15 (1988) 369–379.
[37] L.A. Falls, B.C. Furie, M. Jacobs, B. Furie, A.C. Rigby, J. Biol. Chem. 276 (2001) 23895–23902.
[38] A.P. Demchenko, Eur. Biophys. J. 16 (1988) 121–129.
[39] S. Mukherjee, A. Chattopadhyay, J. Fluoresc. 5 (1995) 237–245.
[40] S. Yamashita, A.G. Szabo, D.T. Krajcarski, N. Yamasaki, Bull. Chem. Soc. Jpn. 62 (1989) 3075–3080.
[41] A. Chattopadhyay, R. Rukmini, FEBS Lett. 335 (1993) 341–344.
[42] S.M. Raja, S.S. Rawat, A. Chattopadhyay, A.K. Lala, Biophys. J. 76 (1999) 1469–1479.
[43] N.C. Santos, M. Prieto, M.A.R.B. Castanho, Biochemistry 37 (1998) 8632–8674.
[44] A. Chattopadhyay, S. Mukherjee, Biochemistry 32 (1993) 3804–3811.
[45] C.E. MacPhee, G.J. Howlett, S.H. Sawyer, A.H.A. Clayton, Biochemistry 38 (1999) 10878–10884.
[46] A.P. Demchenko, N.V. Shcherbatska, Biophys. Chemist. 22 (1985) 131–143.
[47] G.I. King, S.H. White, Biophys. J. 49 (1986) 1047–1054.
[48] T.B. Woolf, B. Roux, Proc. Natl. Acad. Sci. U. S. A. 92 (1994) 11631–11635.
[49] B. Bechinger, J. Seelig, Chem. Phys. Lipids 58 (1991) 1–5.
[50] K.E. Kachel, E. Asuncion-Punzalan, E. London, Biochemistry 34 (1995) 15475–15479.
[51] P.K. Kienker, X. Qiu, S.L. Slatin, A. Finkelstein, K.S. Jakes, J. Membr. Biol. 157 (1997) 27–37.
[52] M. Lindeberg, S.D. Zakharov, W.A. Cramer, J. Mol. Biol. 295 (2000) 679–692.
[53] S.E. Malenbaum, A.R. Merrill, E. London, J. Nat. Toxins 7 (1998) 269–290.
[54] S.D. Zakharov, M. Lindeberg, Y. Griko, Z. Salamon, G. Tollin, F.G. Prendergast, W.A. Cramer, Proc. Natl. Acad. Sci. U. S. A. 95 (1998) 4282–4287.
[55] X.Q. Qui, K.S. Jakes, P.K. Kienker, A. Finkelstein, S.L. Slatin, J. Gen. Physiol. 107 (1996) 313–328.
[56] K.S. Jakes, P.K. Kienker, S.L. Slatin, A. Finkelstein, Proc. Natl. Acad. Sci. U. S. A. 95 (1998) 4321–4326.
[57] L. Raymond, S.L. Slatin, A. Finkelstein, J. Membr. Biol. 84 (1985) 173–181.
[58] O.V. Krasilnikov, J.B. Da Cruz, L.N. Yuldasheva, W.A. Varanda, R.A. Nogueira, J. Membr. Biol. 161 (1998) 83–92.